

Supermassive black holes do not correlate with galaxy disks or pseudobulges

John Kormendy¹, R. Bender^{2,3}, & M. E. Cornell¹

The masses of supermassive black holes are known to correlate with the properties of the bulge components of their host galaxies^{1–5}. In contrast, they appear not to correlate with galaxy disks¹. Disk-grown pseudobulges are intermediate in properties between bulges and disks⁶. It has been unclear whether they do^{1,5} or do not^{7–9} correlate with black holes in the same way that bulges do, because too few pseudobulges were classified to provide a clear result. At stake are conclusions about which parts of galaxies coevolve with black holes¹⁰, possibly by being regulated by energy feedback from black holes¹¹. Here we report pseudobulge classifications for galaxies with dynamically detected black holes and combine them with recent measurements of velocity dispersions in the biggest bulgeless galaxies¹². These data confirm that black holes do not correlate with disks and show that they correlate little or not at all with pseudobulges. We suggest that there are two different modes of black hole feeding. Black holes in bulges grow rapidly to high masses when mergers drive gas infall that feeds quasar-like events. In contrast, small black holes in bulgeless galaxies and galaxies with pseudobulges grow as low-level Seyferts. Growth of the former is driven by global processes, so the biggest black holes coevolve with bulges, but growth of the latter is driven locally and stochastically, and they do not coevolve with disks and pseudobulges.

The well known correlation^{1,5} between dynamically measured BH masses M_{\bullet} and the absolute magnitudes of elliptical galaxies (black points) and the bulge parts of disk galaxies (red points) is shown in Figure 1(b). The correlation has $\chi^2 = 12$ per degree of freedom implying moderate intrinsic scatter. This result and a tighter correlation^{2–5} between M_{\bullet} and host velocity dispersion σ (Figure 2) motivate the idea that BHs and host bulges evolve together and regulate each other^{10,11}. All new results in this paper are in contrast to these two correlations.

Figure 1(a) plots M_{\bullet} versus the absolute magnitude of only the disk part of the host galaxy, with the bulge luminosity removed. We conclude that BHs do not correlate with galaxy disks. This confirms an earlier conclusion¹ based on the more indirect observation that BHs do not correlate with total (bulge + disk) luminosities of disk galaxies. In Figure 1(a), the color of the points—which encodes bulge type (see below)—is irrelevant. A least-squares fit to the red and blue points has correlation coefficient $r = 0.41$. One-sigma errors imply $\chi^2 = 81$ per degree of freedom: the data do not respect the weak anticorrelation. The green points for pure-disk (that is, completely bulgeless) galaxies further confirm the large scatter and lack of correlation.

Figure 1(c) plots M_{\bullet} versus M_K for “pseudobulge” components with disk light removed. They are also included in (b) in ghostly

light blue to show how they compare with classical bulges and ellipticals. Pseudobulges required explanation, as follows.

Much work over several decades has shown that the high-stellar-density central components in disk galaxies – all of which we used to call “bulges” – come in two varieties. How to distinguish them is discussed in the Supplementary Information. The difference was first found observationally but is now understood to be a result of fundamentally different formation mechanisms⁶.

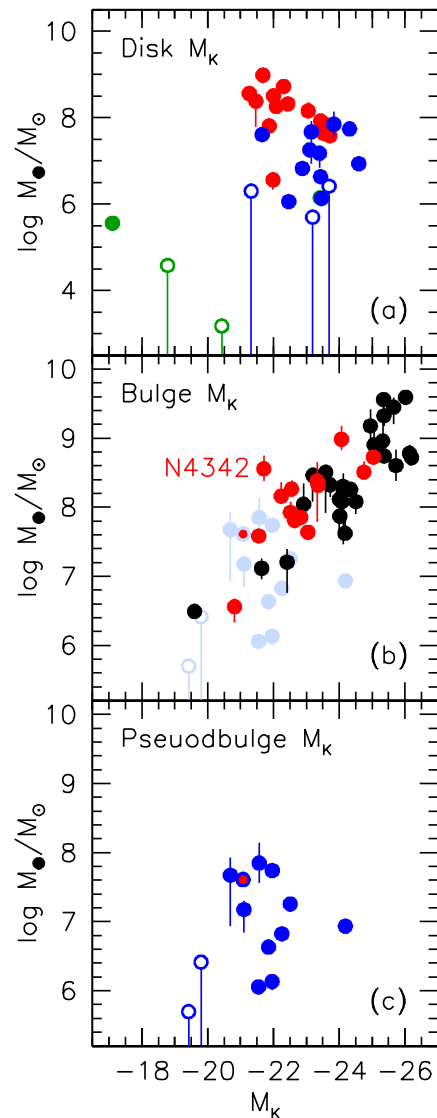


Figure 1 | Correlations of dynamically measured black hole masses M_{\bullet} with the K-band (2.2 μm) absolute magnitude of (a) the disk component with bulge light removed, (b) the bulge with disk light removed, and (c) the pseudobulge with disk light removed. All plotted data are published elsewhere; parameters and sources are discussed in the Supplementary Information, and those for disk galaxies are tabulated there. Elliptical galaxies are plotted in black; classical bulges are plotted in red; pseudobulges are plotted in blue. One galaxy with a dominant pseudobulge but with a possible small classical bulge (NGC 2787) is plotted with a blue symbol that has a red center. In least-squares fits, it is included with the pseudobulges. Error bars are 1 sigma. In panel (b) the red and black points show a good correlation between M_{\bullet} and bulge luminosity; a symmetric, least-squares fit⁴ of a straight line has $\chi^2 = 12.1$ per degree of freedom and a Pearson correlation coefficient of $r = -0.82$. (All χ^2 values quoted in this paper are per degree of freedom.) In contrast, in panel (a), the red and blue points together confirm a previous result¹ that BHs do not correlate with disks: $\chi^2 = 81$ and $r = 0.41$. Green points are for galaxies that contain neither a classical nor a pseudo bulge but only a nuclear star cluster; i.e., these are pure-disk galaxies. They are not included in the above fit, but they strengthen our conclusion. Similarly, in panel (c) the blue points for pseudobulges show no correlation: $\chi^2 = 63$ and $r = 0.27$. In all panels, galaxies that have only M_{\bullet} limits are plotted with open symbols; they were chosen to increase our dynamic range. They, too, support our conclusions. This figure uses K-band magnitudes to minimize effects of star formation and internal absorption, but the Supplementary Information shows that Figure 1 looks essentially the same for V-band (5500 Å) magnitudes.

¹ Department of Astronomy, University of Texas at Austin, 1 University Station, Austin, TX 78712-0259, USA

² Max-Planck-Institut für Extraterrestrische Physik, Giessenbachstrasse, D-85748 Garching-bei-München, Germany

³ Universitäts-Sternwarte, Scheinerstrasse 1, D-81679 München, Germany

Classical bulges (red points in the Figures) are indistinguishable from ellipticals in their structure, velocity distributions, and parameters. Our well developed paradigm is that they formed by galaxy mergers¹³ in our hierarchically clustering universe. Mergers are discrete events separated by long “dead times”, while they happen, their time scales are short; i. e., \approx the crossing time. Gravitational torques scramble disks into ellipticals¹³ and dump large quantities of gas into the center. Observations¹⁴ and theory¹⁵ suggest that the process feeds both starbursts and BHs and causes the latter to grow rapidly in quasar-like events.

Pseudobulges⁶ (blue points in the Figures) are observed to be more disk-like than classical bulges. They are believed to form more gently by the gradual internal redistribution of angular momentum in quiescent galaxy disks. The driving agents are nonaxisymmetries such as bars. One result is the gradual buildup of a high-density central component that can be recognized (Supplementary Information) because it remains rather disk-like. We call these components “pseudobulges” to emphasize their different formation mechanism without forgetting that they look superficially like – and are commonly confused with – classical bulges. The difference from bulges that is most relevant here is this: Gradual gas infall may provide less BH feeding and may drive slower BH growth. One purpose of this paper is to contrast BH–bulge and BH– pseudobulge correlations to look for clues about BH growth mechanisms and the consequent coevolution (or not) of BHs with host galaxies.

With this context, we can interpret Figure 1. Galaxies that contain classical bulges are consistent with the correlations for elliptical galaxies except for one discrepant object (the bulge-dominated S0 galaxy NGC 4342). The implication is that classical bulges and ellipticals coevolve with BHs in the same way. For that coevolution, it is irrelevant that bulges are now surrounded by disks whereas ellipticals are not.

We reach a different conclusion for pseudobulges based on new classifications and measurements of pseudobulge-to-total luminosity ratios for all disk galaxies in our sample⁵ that have dynamical BH detections (Kormendy, in preparation; see the Supplementary Information for a list). A conservative interpretation of Figure 1(b) is that they are roughly consistent with the correlation for classical bulges and ellipticals but have much more scatter. In particular, some pseudobulges deviate from the correlation for ellipticals in having smaller BHs. This was not seen in some previous work^{1,5} because samples were small and because many pseudobulges in BH galaxies had not been classified. But, as published samples have grown larger, the hints have grown stronger that pseudobulges do not correlate with BHs in the same way as classical bulges^{7–9}. We confirm these hints. Particularly compelling is the fact that our galaxies and a new sample of BH detections based on water masers⁹ have no overlap and independently lead to the same conclusion.

Figure 1(c) shows the pseudobulges without guidance from the red and black points. The sample is small, but we have enough dynamic range to conclude that we see no correlation at all. The cumulative amount of BH growth is not extremely different in classical and pseudo bulges, but there is no sign in the correlations that BH feeding has affected the pseudobulges.

The second and more compelling BH–host galaxy correlation is the one between M_{\bullet} and the velocity dispersion σ of the stars at radii where they do not feel the BH gravitationally^{2–5}. Here σ is averaged inside the “effective radius” r_e that contains half of the bulge light. Figure 2 shows this correlation.

As is well known, ellipticals and classical bulges share the same tight correlation. But as in Figure 1, pseudobulges at best show a much larger scatter (Figure 2a). Without the guidance of the red and black points (Figure 2b), they show essentially no correlation. Larger samples that reach smaller M_{\bullet} may show a weak relationship^{16–20}. But we conclude that classical bulges and pseudobulges show very different correlations with M_{\bullet} . The ones for classical bulges are tight enough to suggest coevolution.

Whether pseudobulges correlate with M_{\bullet} with large scatter or not at all, the weakness of any correlation ($r = -0.08$ here) makes no compelling case that pseudobulges and BHs coevolve, beyond the obvious expectation that it is easier to grow bigger BHs and bigger pseudobulges in bigger galaxies that contain more fuel.

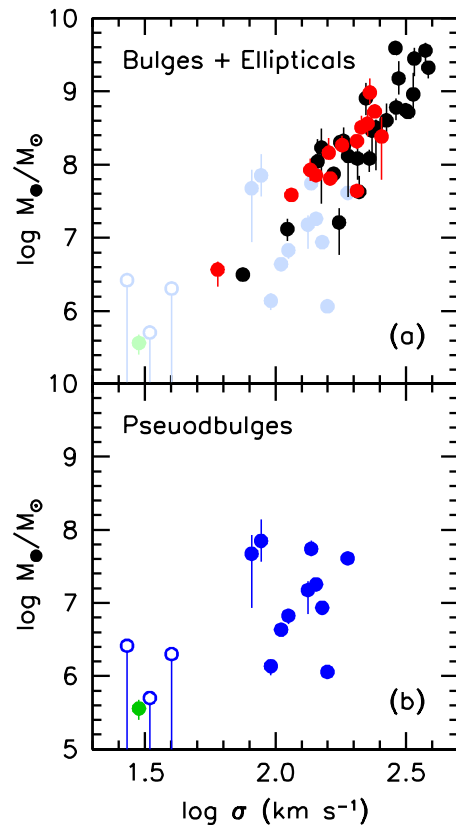


Figure 2 | Correlation of dynamically measured BH masses M_{\bullet} with the velocity dispersion σ of the host elliptical (black points), classical bulge (red points), pseudobulge (blue points), or nuclear star cluster (green point). Date sources are given in the Supplementary Information. Error bars are 1 sigma. The red and black points show the well known $M_{\bullet} - \sigma$ correlation^{2–5}; $\chi^2 = 5.0$ per degree of freedom and $r = 0.89$. Reducing χ^2 to 1.0 implies that the intrinsic scatter in $\log M_{\bullet}$ at fixed σ is 0.26, consistent with previous derivations^{4,5}. This is the tightest correlation between BHs and host galaxy properties and the one that most motivates the idea that BHs and bulges coevolve. In contrast, the blue points for pseudobulges show no correlation: $\chi^2 = 10.4$; $r = -0.08$. This extends suggestions^{7–9} that the BH– σ relation is different for pseudobulges than it is for classical bulges and elliptical galaxies.

From the point of view of galaxy formation by hierarchical clustering, pseudobulge galaxies are already pure-disk galaxies¹². What about even more extreme galaxies that contain neither a classical nor a pseudo bulge? At least some of them contain BHs. Some have active galactic nuclei (AGNs), although these are rare in bulgeless galaxies²¹. And BHs with $M_{\bullet} = 10^4 - 10^6 M_{\odot}$ have confidently been discovered in (pseudo)bulge-less galaxies^{18,21}. The most extreme example is NGC 4395, an Sm galaxy that contains only a tiny, globular-cluster-like nucleus but that has an AGN powered by a BH²² with $M_{\bullet} = (3.6 \pm 1.1) \times 10^5 M_{\odot}$ well measured by reverberation mapping²³. It is the green point with the small error bar in Figure 2. Other such objects include the Sd galaxy NGC 3621²⁴ and the Sph galaxy POX 52, which contains an AGN powered by a BH of mass $M_{\bullet} \approx 10^5 M_{\odot}$ ^{18,25}. Also, it is likely that low- M_{\bullet} AGN samples include bulgeless galaxies,^{16–19} although some are distant and not well resolved.

The lack of correlation of BHs with disks and pseudobulges plus the discovery of BHs in (pseudo)bulgeless galaxies together are critical clues to black hole feeding mechanisms. They motivate the following hypothesis.

We suggest that there are two fundamentally different feeding mechanisms for BHs:

1 – The traditional mechanism is rapid feeding during major mergers when large amounts of gas fall into galaxy centers. We follow other authors^{14,15} who suggest that, at some, perhaps late stage in the merger, the BH grows quickly in a quasar-like event. These are the growth episodes that dominate the waste mass budget of quasar activity^{15,26} that is well explained by the observed density of the biggest BHs in the universe²⁷. In this mode, BH and galaxy growth are controlled by the same global processes and these, we suggest, result in BH – bulge coevolution. If BHs and galaxy formation ever regulate each other¹¹, this is the likely scenario in which it happens.

2 – In contrast, the nuclear activity in bulgeless galaxies is, by and large, weak²¹. Big pseudobulges (NGC 1068 is the highest-luminosity one in Figure 1) can host classical Seyfert nuclei, but there is no sign that these affect global galaxy structure. NGC 1068 is a prototypical oval galaxy⁶ with a prominent pseudobulge that, we believe, formed slowly by inward gas transport in spite of episodic nuclear activity. We suggest that the second mode of BH growth is such weak nuclear activity driven stochastically by local processes that feed gas from $\sim 10^2$ pc where it makes pseudobulges in to the BH. The processes are not understood in detail. But exactly this kind of feeding mode is proposed and modeled in (26); the models suggest that this kind of feeding does not affect galaxy formation. Differences in BH growth and coevolution with host galaxies have also been proposed in studies of the lowest- M_{\bullet} BHs detected mainly via AGN activity^{16,18}. The same scenario can also be reached by studying AGN demographics²⁸. Other recent papers^{29,30} further explore local processes of BH feeding. Figures 1 and 2 tell us that this mode involves little or no coevolution of BHs with any component of the host galaxy.

The seed BHs that grew into today's supermassive BHs are not securely identified. But the smallest BHs grown via local feeding plausibly remain most like those seeds. Since mergers of disk galaxies are believed to make bulges and ellipticals, we suggest that small BHs that are grown by local processes are the seeds of the generally larger BHs that are grown in part by mergers.

Received 12 July 2010.

- Kormendy, J., & Gebhardt, K. Supermassive black holes in galactic nuclei. in *20th Texas Symposium on Relativistic Astrophysics*. (eds Wheeler, J. C., & Martel, H.) 363–381 (AIP, 2001).
- Ferrarese, L., & Merritt, D. A fundamental relation between supermassive black holes and their host galaxies. *Astrophys. J.* **539**, L9–L12 (2000).
- Gebhardt, K., *et al.* A relationship between nuclear black hole mass and galaxy velocity dispersion. *Astrophys. J.* **539**, L13–L16 (2000).
- Tremaine, S. *et al.* The slope of the black hole mass versus velocity dispersion correlation. *Astrophys. J.* **574**, 740–753 (2002).
- Gültekin, K., *et al.* The $M-\sigma$ and $M-L$ relations in galactic bulges, and determinations of their intrinsic scatter. *Astrophys. J.* **698**, 198–221 (2009).
- Kormendy, J., & Kennicutt, R. C. Secular evolution and the formation of pseudobulges in disk galaxies. *Annu. Rev. Astron. Astrophys.* **42**, 603–683 (2004).
- Hu, J. The black hole mass – stellar velocity dispersion correlation: bulges versus pseudo-bulges. *Mon. Not. R. Astron. Soc.* **386**, 2242–2252 (2008).
- Nowak, N., Thomas, J., Erwin, P., Saglia, R. P., Bender, R., & Davies, R. I. Do black hole masses scale with classical bulge luminosities only? The case of the two composite pseudo-bulge galaxies NGC 3368 and NGC 3489. *Mon. Not. R. Astron. Soc.* **403**, 646–672 (2010).
- Greene, J. E., *et al.* Precise black hole masses from megamaser disks: Black hole – bulge relations at low mass. *Astrophys. J.* **721**, 26–45 (2010).
- Ho, L. C., Ed. *Carnegie Observatories Astrophysics Series, Volume 1: Coevolution of Black Holes and Galaxies* (Cambridge Univ. Press, 2004).
- Silk, J., & Rees, M. J. Quasars and galaxy formation. *Astron. Astrophys.* **331**, L1–L4 (1998).
- Kormendy, J., Drory, N., Bender, R., & Cornell, M. E. Bulgeless giant galaxies challenge our picture of galaxy formation by hierarchical clustering. *Astrophys. J.* **723**, 54–80 (2010).
- Toomre, A. Mergers and some consequences. in *Evolution of Galaxies and Stellar Populations* (eds Tinsley, B. M. & Larson, R. B.) 401–426 (Yale University Observatory, 1977).
- Sanders, D. B., Soifer, B. T., Elias, J. H., Madore, B. F., Matthews, K., Neugebauer, G., & Scoville, N. Z. Ultraluminous infrared galaxies and the origin of quasars. *Astrophys. J.* **325**, 74–91 (1988).
- Hopkins, P. F., Hernquist, L., Cox, T. J., di Matteo, T., Robertson, B., & Springel, V. A unified, merger-driven model of the origin of starbursts, quasars, the cosmic X-ray background, supermassive black holes, and galaxy spheroids. *Astrophys. J. Suppl. Ser.* **163**, 1–49 (2006).
- Barth, A. J., Greene, J. E., & Ho, L. C. Dwarf Seyfert 1 nuclei and the low-mass end of the $M_{\text{BH}} - \sigma$ relation. *Astrophys. J.* **619**, L151–L154 (2005).
- Greene, J. E., & Ho, L. C. The $M_{\text{BH}} - \sigma_*$ relation in local active galaxies. *Astrophys. J.* **641**, L21–L24 (2006).
- Greene, J. E., Ho, L. C., & Barth, A. J. Black holes in pseudobulges and spheroidals: A change in the black hole – bulge scaling relations at low mass. *Astrophys. J.* **688**, 159–179 (2008).
- Bentz, M. C., Peterson, B. M., Pogge, R. W., & Vestergaard, M. The black hole mass – bulge luminosity relationship for active galactic nuclei from reverberation mapping and *Hubble Space Telescope* imaging. *Astrophys. J.* **694**, L166–L170 (2009).
- Woo, J.-H., *et al.* The Lick AGN monitoring project: The $M_{\text{BH}} - \sigma_*$ relation for reverberation-mapped active galaxies. *Astrophys. J.* **716**, 269–280 (2010).
- Ho, L. C. Nuclear activity in nearby galaxies. *Annu. Rev. Astron. Astrophys.* **46**, 475–539 (2008).
- Filippenko, A. V., & Ho, L. C. A low-mass central black hole in the bulgeless Seyfert 1 galaxy NGC 4395. *Astrophys. J.* **588**, L13–L16 (2003).
- Peterson, B. M., *et al.* Multiwavelength monitoring of the dwarf Seyfert 1 galaxy NGC 4395. I. A Reverberation-based measurement of the black hole mass. *Astrophys. J.* **632**, 799–808 (2005).
- Barth, A. J., Strigari, L. E., Bentz, M. C., Greene, J. E., & Ho, L. C. Dynamical constraints on the masses of the nuclear star cluster and black hole in the late-type spiral galaxy NGC 3621. *Astrophys. J.* **690**, 1031–1044 (2009).
- Thornton, C. E., Barth, A. J.; Ho, L. C.; Rutledge, R. E., & Greene, J. E. The host galaxy and central engine of the dwarf active galactic nucleus POX 52. *Astrophys. J.* **686**, 892–910 (2008).
- Hopkins, P. F., & Hernquist, L. Fueling low-level AGN activity through stochastic accretion of cold gas. *Astrophys. J. Suppl. Ser.* **166**, 1–36 (2006).
- Yu, Q., & Tremaine, S. Observational constraints on growth of massive black holes. *Mon. Not. R. Astron. Soc.* **335**, 965–976 (2002).
- Schawinski, K., *et al.* Galaxy zoo: The fundamentally different co-evolution of supermassive black holes and their early- and late-type host galaxies. *Astrophys. J.* **711**, 284–302 (2010).
- Kumar, P., & Johnson, J. L. Supernovae-induced accretion and star formation in the inner kiloparsec of a gaseous disc. *Mon. Not. R. Astron. Soc.* **404**, 2170–2176 (2010).
- Hopkins, P. F., & Quataert, E. How do massive black holes get their gas? *Mon. Not. R. Astron. Soc.* **407**, 1529–1564 (2010).

Supplementary Information is linked to the online version of the paper at www.nature.com/nature.

Acknowledgments We acknowledge with pleasure the collaboration of Niv Drory on work¹² leading up to this paper. We thank Niv and Jenny Greene for helpful comments on the MS and Jenny for communicating the maser BH detection results before publication⁹. We also thank Karl Gebhardt for permission to use M_{\bullet} for NGC 4736 and NGC 4826 and John Jardel for permission to use his updated M_{\bullet} for NGC 4594 before publication. Some data used here were obtained with the Hobby-Eberly Telescope (HET). It is a joint project of the University of Texas at Austin, Pennsylvania State University, Stanford University Ludwig-Maximilians-Universität Munich, and Georg-August-Universität Göttingen. The HET is named in honor of its principal benefactors, William P. Hobby and Robert E. Eberly. We made extensive use of data from the Two Micron All Sky Survey, a joint project of the University of Massachusetts and the Infrared Processing and Analysis Center/California Institute of Technology funded by NASA and by the NSF. We also made extensive use of the NASA/IPAC Extragalactic Database (NED), which is operated by Caltech and JPL under contract with NASA, of the HyperLeda database <<http://leda.univ-lyon1.fr>>, and of NASA's Astrophysics Data System bibliographic services. Finally, we are grateful to the National Science Foundation for grant support.

Author Contributions J.K. led the program, carried out the analysis for this paper and wrote most of the text. M.E.C. oversaw the HET observations, preprocessed the HET spectra, and provided technical support throughout the project. R.B. calculated the velocity dispersions from the HET spectra and made all least-squares fits. All authors contributed to the writing of this paper.

Author Information Reprints and permissions information is available at www.nature.com/reprints. The authors declare no competing financial interests. Correspondence and requests for materials should be addressed to J.K. (kormendy@astro.as.utexas.edu).

Supplementary Information

The first section summarizes the differences between classical bulges and pseudobulges and lists the criteria that we use to distinguish them. The second section tabulates the data used in the construction of the figures in the main text. The third section shows a V-band version of Figure 1.

Internal Secular Evolution of Disk Galaxies and the Distinction Between Classical and Pseudo Bulges

The distinction between classical bulges and pseudobulges plays a critical role in the main text. It is not yet securely a part of the extragalactic folklore, so we review it briefly:

Classical bulges: Our standard picture for the formation of elliptical galaxies by major galaxy mergers in the context of hierarchical clustering was summarized in the main text. Classical bulges have observed properties that are similar to those of comparably low-luminosity ellipticals and are believed to have formed like ellipticals in major mergers. Renzini³¹ clearly states the usual interpretation of classical bulges: “It appears legitimate to look at bulges as ellipticals that happen to have a prominent disk around them [and] ellipticals as bulges that for some reason have missed the opportunity to acquire or maintain a prominent disk.” This story is well known.

Pseudobulges are less well known. Kormendy & Kennicutt review⁶ a large body of evidence that, between major merger events, galaxy disks evolve continually and slowly (“secularly”) as nonaxisymmetries transfer angular momentum outward. The main driving agents are bars, globally oval disks^{6,32,33}, and global spiral structure that reaches the center of the galaxy. The result is a variety of well known structural features such as outer rings, inner rings that encircle the ends of bars, and pseudobulges. The latter were first recognized^{33,34} because they are more disk-like than are classical bulges. More recent work confirms and greatly extends this distinction⁶. In parallel, theoretical work has shown that disks fundamentally rearrange their angular momentum distributions in a way that dumps large quantities of gas into the center. There, it is expected and observed to feed starbursts and to build high-density components – we infer: the observed pseudobulges – that were made slowly out of disk material and not quickly in a merger. The distinction is important here because mergers are thought to feed BHs rapidly^{14,15}. It therefore becomes important to ask whether these two very different ways to form bulge-like central components do or do not grow BHs similarly. We confirm previous suggestions^{7–9} that they do not. In fact, we find no BH – pseudobulge correlations at all. This suggests that BHs coevolve only with classical bulges and ellipticals – i. e., only with remnants of major mergers.

The key to recognizing pseudobulges is that they “remember” their disk origins. They continue to have structural, dynamical, and star formation properties that are more like those of their associated disks than they are like those of ellipticals and classical bulges. The criteria used to classify bulges as pseudo or classical are listed in the Kormendy & Kennicutt review⁶ and in the paper in preparation on BH hosts. Here is a brief summary; justification is given in the above papers:

1 – Pseudobulges often have disky structure – their apparent flattening is similar to that of the outer disk, or they contain spiral structure that reaches all the way in to the galaxy center. Classical bulges look much rounder than their disks unless the galaxy is seen face-on. They cannot show spiral structure.

2 – In relatively face-on galaxies the presence of a nuclear bar implies a pseudobulge. Bars are purely disk phenomena.

3 – In edge-on galaxies, boxy bulges are edge-on bars; seeing one is sufficient grounds for identifying a pseudobulge.

4 – Most pseudobulges have Sérsic³⁵ index $n < 2$, whereas almost all classical bulges have $n \geq 2$. Here n is a parameter of the projected brightness profile, $\log I \propto \text{radius}^{1/n}$.

5 – In pseudobulges, ordered motions (rotation) are slightly more important with respect to random motions (σ) than they are in classical bulges. This is even more true in disks.

6 – Many pseudobulges are low- σ outliers in the well known correlation³⁶ between (pseudo)bulge luminosity and σ . Frequently, σ decreases inward in the central few arcsec.

7 – If the center of the galaxy is dominated by gas, dust, and star formation but there is no sign of a merger in progress, then the bulge is at least mostly pseudo.

8 – Small bulge-to-total luminosity ratios do not guarantee that a bulge is pseudo, but if $B/T \gtrsim 0.5$, then the bulge is classical.

Table of Data for Disk Galaxies Shown in Figures

Supplementary Table 1 lists the data for the disk galaxies that are included in Figures 1 and 2. It is an excerpt from a more detailed table in a paper (Kormendy, in preparation) on BH host galaxies. Most references for parameter sources are given there; exceptions are as follows: The galaxy sample, BH masses, and parameters not otherwise credited are from the recent study of M_{\bullet} correlations by Gültekin⁵. They include σ , which is tabulated in Gültekin’s paper as the mean velocity dispersion inside approximately the “effective radius” r_e that contains half of the light of the bulge. Note: Only disk galaxies are included in the table. Parameters for ellipticals are given in Gültekin’s paper. BH mass limits in essentially (pseudo)bulge-less galaxies are from paper (12).

The table is divided into two parts, galaxies with classical bulges and then galaxies with pseudobulges. Column (8) lists which of the criteria in the previous section led to the bulge classifications in Columns (6) and (7).

Photometric decomposition of brightness distributions into (pseudo)bulge and disk components is discussed for each galaxy in the paper in preparation on BH hosts. Fifteen of the 25 galaxies in the table have $(P)B/T$ measurements from 2 – 7 independent sources. Ten have only one source; seven of these are measured in the BH hosts paper. A variety of techniques are used in published papers; most of them use Sérsic functions for bulges and exponentials for disks. The decompositions in the BH hosts paper are based on composite brightness profiles from as many sources as possible. Most of them are measured in the above paper. They include HST profiles whenever possible. No $(P)B/T$ ratio is seriously compromised by the lack of HST data. The BH hosts paper uses one-dimensional Sérsic-exponential decompositions of major-axis profiles but takes ellipticity profiles fully into account in calculating $(P)B/T$.

SUPPLEMENTARY TABLE 1
PARAMETERS OF DISK GALAXIES WITH DYNAMICALLY DETECTED SUPERMASSIVE BLACK HOLES

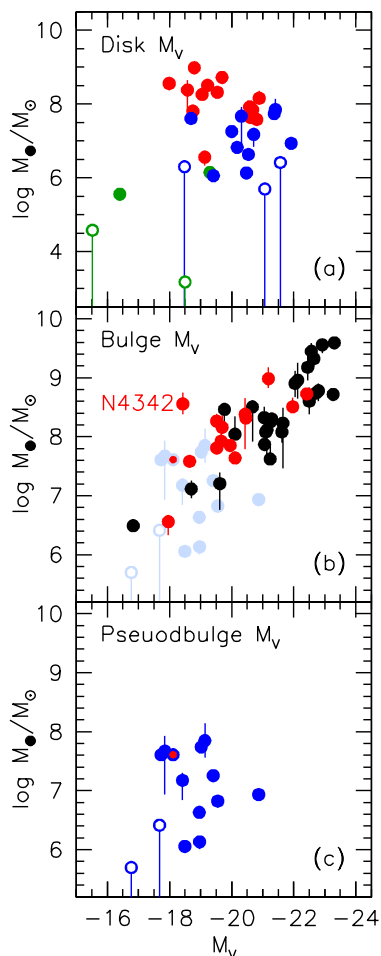
Galaxy	Type	D (Mpc)	M_V	M_K	B/T	PB/T	(Pseudo)bulge criteria	σ (km s^{-1})	V_{circ} (km s^{-1})	M_{\bullet} (M_{\odot})
(1)	(2)	(3)	(4)	(5)	(6)	(7)	(8)	(9)	(10)	(11)
M 31	Sb	0.77	−21.20	−23.48	0.25 V ; 0.32 K	0	1,4,5	160 ± 8	250 ± 20	1.44 (1.16–2.31) × 10 ⁸
M 81	Sab	3.63	−21.13	−24.00	0.34 ± 0.02	0	1,4	143 ± 7	240 ± 10	7.08 (6.11–8.85) × 10 ⁷
NGC 1023	SB0	11.4	−21.14	−24.07	0.39 ± 0.01	0:	1,4,5	205 ± 14	251 ± 15	4.35 (3.87–4.82) × 10 ⁷
NGC 3115	S0/	10.2	−21.30	−24.18	0.90 ± 0.02	~ 0	1,4,5,8	230 ± 11	315 ± 10	9.6 (6.7–15) × 10 ⁸
NGC 3245	S0	20.9	−20.85	−23.75	0.70 ± 0.02	0:	4,8	205 ± 10	290 ± 5	2.1 (1.6–2.6) × 10 ⁸
NGC 3585	S0/	20.0	−22.05	−24.83	0.93	0:	1,4,5,8	213 ± 10	280 ± 20	3.22 (2.65–4.63) × 10 ⁸
NGC 3998	S0	14.9	−20.62	−23.51	0.85	0:	4,8	255 ± 50	408 ± 42	2.4 (0.6–4.5) × 10 ⁸
NGC 4026	S0/	13.6	−20.06	−23.09	0.61 ± 0.07	0:	1,4,8	180 ± 9	255 ± 10	1.83 (1.48–2.44) × 10 ⁸
NGC 4258	SABbc	7.3	−20.95	−23.85	0.12 ± 0.02	0:	1,4,5	115 ± 10	208 ± 6	3.82 (3.81–3.83) × 10 ⁷
NGC 4342	S0	18.0	−18.98	−22.26	0.60 ± 0.05	0.015	1,4,8	225 ± 11	311 ± 10	3.6 (2.4–5.6) × 10 ⁸
NGC 4564	S0	15.9	−19.96	−23.08	0.67 ± 0.04	0:	1,4,8	162 ± 8	229 ± 2	6.43 (5.50–6.81) × 10 ⁷
NGC 4594	Sa	10.3	−22.50	−25.12	0.93 ± 0.01	0.01	1,4,5,8	240 ± 12	359 ± 10	5.3 (4.74–6.08) × 10 ⁸
NGC 4596	SB0/a	18.0	−20.97	−23.82	0.30 ± 0.05	0:	1,4,5	136 ± 6	230 ± 30	8.4 (5.9–12) × 10 ⁷
NGC 7457	S0	12.4	−19.45	−22.31	0.25	0:	1,4,5	60 ± 3	105 ± 5	3.63 (2.13–4.69) × 10 ⁶
Galaxy	SBbc	0.008	−20.8	−23.7	0:	0.19 ± 0.02	3,5,7	105 ± 20	220 ± 20	4.30 (3.94–4.66) × 10 ⁶
Circinus	SABb:	2.8	−19.80	−22.85	0:	0.30 ± 0.03	4,7	158 ± 18	155 ± 10	1.19 (0.98–1.47) × 10 ⁶
NGC 1068	Sb	15.4	−22.18	−25.16	0:	0.30 V ; 0.41 K	2,4,7	151 ± 7	321 ± 22	8.6 (8.3–8.9) × 10 ⁶
NGC 1300	SBbc	20.1	−21.54	−23.96	0:	0.11 ± 0.02	4,7	88 ± 3	220 ± 10	7.1 (3.6–14) × 10 ⁷
NGC 2748	Sc	24.9	−20.42	−23.26	0	0.094 ± 0.012	4,7	81 ± 1	150 ± 10	4.7 (0.86–8.5) × 10 ⁷
NGC 2787	SB0/a	7.5	−19.19	−22.16	0.11	0.26 ± 0.02	1,4,5	189 ± 9	225 ± 10	4.07 (3.60–4.45) × 10 ⁷
NGC 3227	SBa	17.0	−20.84	−23.52	0:	0.11 ± 0.03	4,7	133 ± 12	250 ± 10	1.5 (0.7–2.0) × 10 ⁷
NGC 3384	SB0	11.7	−20.50	−23.60	0.0043	0.36 ± 0.02	1,2,4,5	143 ± 7	156 ± 10	1.8 (1.5–1.9) × 10 ⁷
NGC 4736	Sab	4.9	−20.66	−23.37	0:	0.36 ± 0.01	2,4,5,7	112 ± 3	181 ± 10	6.68 (5.14–8.22) × 10 ⁶
NGC 4826	Sab	6.4	−20.72	−23.71	0:	0.20 ± 0.05	5,6,7	96 ± 3	155 ± 5	1.36 (1.02–1.71) × 10 ⁶
NGC 7582	SBab	22.3	−21.49	−24.43	0:	0.10 ± 0.01	4,7	137 ± 20	226 ± 10	5.5 (4.4–7.1) × 10 ⁷

NOTE.— The list is divided into two groups, (*top*) galaxies with classical bulges, and (*bottom*) galaxies with dominant pseudobulges. Galaxies with M_{\bullet} limits are not listed but are from references (12), (37), (38), and (39). The filled green circles in Figures 1 and 2 are the Sm galaxy NGC 4395²³ and the Scd galaxy NGC 4945⁴⁰. Column (2): Hubble types are mostly from the RC3⁴¹. Column (3): Adopted distance, mostly from Gültekin⁵. Column (4): Total galaxy absolute magnitudes M_V are calculated from apparent integrated magnitudes from Hyperleda⁴² or RC3 and colors (preferably $(B-V)_T$ from RC3, otherwise from Hyperleda). Galactic absorptions are from Schlegel⁴³. Column (5): Total galaxy absolute magnitude in K band; K_T total apparent magnitudes are from the 2MASS⁴⁴ Large Galaxy Atlas⁴⁵ or from the 2MASS online extended source catalog. Columns (6) and (7) are averages of measured classical-bulge-to-total and pseudobulge-to-total luminosity ratios. Quoted errors are from the variety of decompositions discussed in the BH hosts paper or, when there are multiple sources, are the dispersions in the published values divided by the square root of the number of values averaged. In the latter case, the smallest values are unrealistically optimistic estimates of the true measurement errors and indicate fortuitously good agreement between published values. Colons indicate uncertainty in the sense that we know of no observational evidence that this component is present in the galaxy but we are also not aware of a rigorous proof that a small contribution by this component is impossible. Different $(P)B/T$ values in V band and in K band are measured and listed for M 31 and NGC 1068. Tiny values of PB/T in bulge-dominated galaxies are measures of nuclear disks. We list $B/T = 0.0043$ for NGC 3384; this refers to a tiny central component that formally satisfies the criteria for classical bulges, but it is more likely to be a stellar nucleus. Bulge absolute magnitudes are $M_V - 2.5 \log B/T$ or $M_V - 2.5 \log PB/T$. Similarly, disk absolute magnitudes are $M_V - 2.5 \log(1 - B/T)$ or $M_V - 2.5 \log(1 - PB/T)$. If both B/T and PB/T are non-zero, then the total magnitude is corrected for both the bulge and the pseudobulge to get the disk magnitude. Column (8): Criteria used to classify the bulge as classical or pseudo as discussed in the text. Column (9): Velocity dispersion σ averaged inside r_e for the (pseudo)bulge, from reference (5). Column (10): Circular rotation velocity at large radii, V_{circ} , corrected to edge-on inclination. In many galaxies (e.g., M 31) error bars reflect variations with radius, not errors of measurement. Column (11): Measured BH mass M_{\bullet} , mostly from reference (5). For NGC 4594, M_{\bullet} is from Jardel et al. 2010, in preparation; for our Galaxy, M_{\bullet} is from reference (50), and for NGC 4736 and NGC 4826, M_{\bullet} is from Gebhardt et al. 2010, in preparation. When we used a different distance than the source of M_{\bullet} did, we quote three significant figures for M_{\bullet} . This is only so that we do not lose precision; three figures are clearly not significant. Parameters whose sources are not given here are from a paper in preparation on BH host galaxies.

For giant ellipticals, published estimates of M_{\bullet} that are based on stellar dynamics need correction for the effects of triaxiality and for the effect of including halo dark matter (DM) in the models. These corrections are mostly relevant only for the biggest ellipticals, i. e., the ones that we believe were formed by dry mergers⁴⁶. Including DM inevitably increases M_{\bullet} estimates, and so far, including triaxiality has had the same effect. Corrected M_{\bullet} values are available for three ellipticals: NGC 3379⁴⁷, NGC 4486⁴⁸, and NGC 4649⁴⁹. The corrected masses are factors of ~ 2 larger than those used in the figures. This does not effect our conclusions. But it artificially increases the scatter. Until more corrections are available, we decided to be consistent and used the Gültekin tabulated masses⁵.

V-Band Version of Figure 1

Supplementary Figure 1 shows a version of Figure 1 that is based on optical (V-band) absolute magnitudes rather than infrared absolute magnitudes. We noted in the Figure 1 caption that we used K-band magnitudes there because they minimize effects of star formation and internal absorption. However, the present figure based on V-band magnitudes looks virtually identical to Figure 1 and leads to the same conclusions. This means that variations in mass-to-light ratios for these galaxies, some or which are actively forming stars and others of which are not, do not affect our results.



Supplementary Figure 1 | Correlations of dynamically measured BH mass M_{\bullet} with (a) disk, (b) classical bulge, and (c) pseudobulge absolute magnitude in V band (5500 Å). Elliptical galaxies are plotted with black points; classical bulges are plotted in red, and pseudobulges are plotted in blue. Panel (b) also shows the pseudobulges in light blue. Green points are for galaxies that contain neither a classical nor a pseudo bulge but only a nuclear star cluster. Open circles show galaxies with BH mass limits.

Acknowledgments

This work was supported by the National Science Foundation under grant AST-0607490.

References

31. Renzini, A. 1999. Origin of bulges. in *The Formation of Galactic Bulges*, (eds. Carollo, C. M., Ferguson, H. C., & Wyse, R. F. G.) 9–25 (Cambridge University Press, 1999)
32. Kormendy, J., & Norman, C. A. Observational constraints on driving mechanisms for spiral density waves. *Astrophys. J.* **233**, 539–552 (1979).
33. Kormendy, J. Observations of galaxy structure and dynamics. in *12th Saas-Fee Course, Morphology and dynamics of galaxies.*, (eds. Martinet, L., & Mayor, M.) 113–288 (Geneva Observatory, 1982)
34. Kormendy, J. Kinematics of extragalactic bulges: Evidence that some bulges are really disks. in *IAU Symposium 153, Galactic Bulges* (eds. Dejonghe, H., & Habing, H. J.) 209–228 (Kluwer, 1993)
35. Sérsic, J. L. *Atlas de Galaxias Australes*. (Observatorio Astronómico, Universidad Nacional de Córdoba, 1968)
36. Faber, S. M., & Jackson, R. E. Velocity dispersions and mass-to-light ratios for elliptical galaxies. *Astrophys. J.* **204**, 668–683 (1976).
37. Gebhardt, K., *et al.* M33: A galaxy with no supermassive black hole. *Astron. J.* **122**, 2469–2476 (2001).
38. Böker, T., van der Marel, R. P., & Vacca, W. D. CO band head spectroscopy of IC 342: Mass and age of the nuclear star cluster. *Astron. J.* **118**, 831–842 (1999).
39. Valluri, M., Ferrarese, L., Merritt, D., & Joseph, C. L. The low end of the supermassive black hole mass function: Constraining the mass of a nuclear black hole in NGC 205 via stellar kinematics. *Astrophys. J.* **628**, 137–152 (2005).
40. Greenhill, L. J., Moran, J. M., & Herrnstein, J. R. The distribution of H₂O maser emission in the nucleus of NGC 4945. *Astrophys. J.* **481**, L23–L26 (1997).
41. de Vaucouleurs, G., de Vaucouleurs, A., Corwin, H. G., Buta, R. J., Paturel, G., & Fouqué, P. *Third Reference Catalogue of Bright Galaxies*. (Springer, 1991).
42. Paturel, G., Petit, C., Prugniel, Ph., Theureau, G., Rousseau, J., Brouty, M., Dubois, P., & Cambrésy, L. HYPERLEDA. I. Identification and designation of galaxies. *Astron. Astrophys.* **412**, 45–55 (2003).
43. Schlegel, D. J., Finkbeiner, D. P., & Davis, M. Maps of dust infrared emission for use in estimation of reddening and cosmic microwave background radiation foregrounds. *Astrophys. J.* **500**, 525–553 (1998).
44. Skrutskie, M. F., *et al.* The two micron all sky survey (2MASS). *Astron. J.* **131**, 1163–1183 (2006).
45. Jarrett, T. H., Chester, T., Cutri, R., Schneider, S. E., & Huchra, J. P. The 2MASS Large Galaxy Atlas. *Astron. J.* **125**, 525–554 (2003).
46. Kormendy, J., Fisher, D. B., Cornell, M. E., & Bender, R. Structure and formation of elliptical and spheroidal galaxies. *Astrophys. J. Suppl. Ser.* **182**, 216–309 (2009).
47. van den Bosch, R. C. E., & de Zeeuw, P. T. Estimating black hole masses in triaxial galaxies. *Mon. Not. R. Astron. Soc.* **401**, 1770–1780 (2010).
48. Gebhardt, K., & Thomas, J. The black hole mass, stellar mass-to-light ratio, and dark halo in M87. *Astrophys. J.* **700**, 1690–1701 (2009).
49. Shen, J., & Gebhardt, K. The supermassive black hole and dark matter halo of NGC 4649 (M60). *Astrophys. J.* **711**, 484–494 (2010).
50. Genzel, R., Eisenhauer, F., & Gillessen, S. The massive black hole and nuclear star cluster in the center of the Milky Way. *Rev. Mod. Phys.*, in press; preprint at <<http://arxiv.org/abs/1006.0064>> (2010).